

# Investigation of corrosion resistant mixed oxide-based anode and cathode Pt catalysts: Effect of the composition on the electrocatalytic performance

Laboratory Project II

**Khirdakhanim Salmanzade**

Supervisor: Dr. András Tompos

Consultants: Dr. Irina Borbáth

Renewable Energy Research Group

Institute of Materials and Environmental Chemistry

Research Centre for Natural Sciences



Internal consultant: Dr. Imre Miklós Szilágyi; associate professor



Budapest University of Technology and Economics

Faculty of Chemical Technology and Biotechnology

Department of Inorganic and Analytical Chemistry

## Contents

1. Introduction.....	3
1.1. TiO <sub>2</sub> -rutile-based mixed oxide – active carbon composite supported Pt electrocatalysts .....	3
1.2. Peculiarities of Nb-containing TiO <sub>2</sub> -based composite supported Pt electrocatalysts .....	4
1.3. Application of NiWO <sub>4</sub> -based composite supported Pt catalysts as anode and cathode in PEM fuel cell.....	6
2. Experimental .....	7
2.1. Electrocatalysts used.....	7
2.2. Preparation of the 20 and 40 wt.% Pt electrocatalysts.....	10
2.3. Electrochemical characterization .....	11
2.3.1. Electrochemical characterization by cyclic voltammetry .....	11
2.3.2. Electrochemical characterization by ORR.....	11
2.3.3. Electrochemical characterization by HOR.....	12
3. Results and discussion .....	12
3.1. Electrochemical characterization of the Pt/Ti <sub>0.8</sub> Mo <sub>0.2</sub> O <sub>2</sub> -C anode electrocatalysts .....	12
3.2. Electrochemical characterization of mixed oxide-containing cathode catalysts .....	16
3.3. Electrochemical characterization of the scaled-up materials.....	17
4. Summary .....	20
5. References.....	21

## 1. Introduction

A novel class of electrocatalysts proposed for use in Polymer Electrolyte Membrane (PEM) fuel cells comprises Pt catalysts supported on titanium dioxide doped with certain transition metals (e.g., W, Mo, Nb, Ta and Sn) [1] [2] [3] [4] [5] [6] [7] [8] [9]. These catalysts are developed to overcome the inherent limitations of the traditional CO- and corrosion-sensitive Pt/C catalysts. The corrosion of carbon, sintering and dissolution of Pt nanoparticles in acidic media are well known phenomena leading to activity loss [10] [11]. The consequence of both processes is the loss of the active surface of the catalysts. Since the electrocatalyst is responsible for roughly 30% of the price of a PEM fuel cell [12], more corrosion resistant electrocatalysts with decreased Pt content are inevitable for ensuring the economic viability of the PEM fuel cell technology.

The key requirements for prospective electrocatalysts in PEM fuel cells involve [13]: (i) high stability in the anticipated pH/potential window, (ii) high resistance against electrochemical corrosion, (iii) good electronic and proton conductivity, (iv) high specific surface area, (v) appropriate porosity for mass transfer of liquid fuels or oxygen gas and the minimization of water flooding in electrodes, and (vi) strong interaction between the Pt nanoparticles and the support. In the last decade a range of oxide containing electrocatalyst materials were proposed for both the hydrogen oxidation reaction (HOR) and the oxygen reduction reaction (ORR). Because of the strong metal-support interaction (SMSI) the metal oxides are also capable to stabilize active metal in highly dispersed state, and might help to suppress Pt dissolution on oxygen reduction cathodes at open-circuit potentials (OCP) or in the start-up-shut-down driving of electric vehicles. In addition, oxide substrates are not prone to oxidation and degradation, as are carbon supports. However, even if in electrochemical experiments many of them showed excellent properties, their utilization in PEMFCs remains extremely rare.

### 1.1 TiO<sub>2</sub>-rutile-based mixed oxide – active carbon composite supported Pt electrocatalysts

The concept of non-noble metal-doped TiO<sub>2</sub> – active carbon composite supports, developed in the *Renewable Energy Research Group* (RERG), is based on the idea of bringing together the excellent stability and nanoparticle-stabilizing ability of TiO<sub>2</sub> with the good co-catalytic properties of doping metal (M= W, Mo, Nb and Sn) and with the good conductivity and large surface area of active carbon in a unique material system. It has been demonstrated [14] [15] that exclusive incorporation of the doping metals into substitutional sites of the TiO<sub>2</sub> lattice is a

necessary requirement for practical realization of a mixed oxide – active carbon composite as a support for electrocatalysts in PEM fuel cells. Under such circumstances the TiO<sub>2</sub> lattice protects the doping metal atoms from dissolution, while they can still provide CO tolerance [16] [17] [18] [19] [20]. Better performance of the Pt/Ti<sub>0.7</sub>Mo<sub>0.3</sub>O<sub>2</sub>-C (M= W, Mo) catalysts in a single cell test device using hydrogen containing 100 ppm CO compared to the reference Pt/C and PtRu/C catalysts was also demonstrated [21].

In Ref. [22] an optimized route for preparation of novel TiO<sub>2</sub>-rutile-based Ti<sub>0.8</sub>Mo<sub>0.2</sub>O<sub>2</sub>-C multifunctional composite support materials with different mixed oxide/carbon ratio (Ti<sub>0.8</sub>Mo<sub>0.2</sub>O<sub>2</sub>/C= 75/25, 50/50 and 25/75) was elaborated using Vulcan XC-72, unmodified (BP) and functionalized Black Pearls 2000 (F-BP) carbon materials. A multistep sol-gel-based synthesis method was also adapted to obtain composite materials based on exfoliated graphite oxide (GO) with 25 wt.% GO and rutile-TiO<sub>2</sub> structure. As demonstrated by X-ray diffraction, by using the optimized synthesis route, almost complete Mo incorporation was achieved, in spite of the widely differing structural and surface chemical characteristics of the carbon materials.

The electrochemical results indicate that (i) there are characteristic performance differences between the electrocatalysts with different mixed oxide/carbon ratio, and (ii) the catalytic properties of the system are mainly determined by the Pt-Mo interactions. Thus, an increase of the mixed oxide content in composites to 50 and 75 wt.%, leading to a pronounced enhancement of Pt-Mo interactions, results to better tolerance of the catalysts to CO as compared to those with high carbon content. However, the more homogeneous microstructure of the catalysts with high carbon content (75 wt.%) seems to be the key for enhanced long-term stability. Considering also the fact that high oxide content in the catalyst layer can lead to a slight increase of the cell resistance, the BP- and F-BP-based Pt electrocatalysts with Ti<sub>0.8</sub>Mo<sub>0.2</sub>O<sub>2</sub>/C= 25/75 ratio seems to be more promising for general use.

## **1.2 Peculiarities of Nb-containing TiO<sub>2</sub>-based composite supported Pt electrocatalysts**

Niobium oxides are an interesting n-type semiconductors [23], which has found important applications in electronics and optical applications, including thin films (antireflective coatings, solar control, etc. [24]). Nb is known to be the most promising dopant used to enhance electrical conductivity of titania [25] [26] [27] since the similarity of the Pauling ionic radii of Nb<sup>5+</sup> (r= 0.70 Å) and Ti<sup>4+</sup> (r= 0.68 Å) in sixfold coordination results in almost no lattice distortion [28].

Different approaches have been reported in the literature to improve the electrical conductivity of TiO<sub>2</sub> including doping with niobium and followed by heat treatment at high temperatures under a reducing atmosphere. Thus, it has been reported [29] that Nb-doped TiO<sub>2</sub> (0.65 atomic% Nb) exhibits metallic-type conduction upon annealing of the specimen at elevated temperatures (800-950 °C) in the gas phase of very low oxygen activities ( $10^{-11}$  Pa  $< p_{O_2} < 10^{-8}$  Pa).

X-ray diffraction analyses revealed that upon doping of TiO<sub>2</sub> with Nb niobium hinders the anatase-to-rutile transformation and prevents the grain growth [30], which is important to achieve a conductive support with high specific surface area. This might be due to Nb<sup>5+</sup> species substituting for Ti<sup>4+</sup> in the crystalline lattice [31], reducing the oxygen vacancy concentration in titania [32].

Valigi *et al.* [33] studied the Nb<sub>x</sub>Ti<sub>(1-x)</sub>O<sub>2</sub> system in the composition range  $0.0 < x < 0.1$  for different heat treatment conditions. The effect of the various incorporated species on the TiO<sub>2</sub> unit-cell volume was discussed. The results show that for the samples prepared in vacuum, niobium is incorporated as Nb<sup>5+</sup> compensated by an equivalent amount of Ti<sup>3+</sup>. If the treatment was done in air, the maximum solubility of Nb<sup>5+</sup> into rutile form was 6.6 Nb atoms/100 Ti atoms, above which Nb excess was segregated as a ternary phase TiNb<sub>2</sub>O<sub>7</sub>. On subsequent heating in air the Ti<sup>3+</sup> was oxidized to Ti<sup>4+</sup> yielding a compensation of Nb<sup>5+</sup> by cation vacancies. The secondary phase of TiNb<sub>2</sub>O<sub>7</sub> has been also observed by Zakrzewska *et al.* [34] when Nb content exceeded 6 atomic%.

Design and preparation of the Nb-containing metal oxide-supported Pt electrocatalysts for the ORR have been extensively studied. It has been demonstrated in Ref. [35] that the dopant may not only increase the electrical conductivity of TiO<sub>2</sub> but also modify the Pt fine structure, resulting in the modification of the ORR activity. Sasaki *et al.* [36] demonstrated that niobium oxide nanoparticles could be adequate support for Pt, reducing at the same time the noble-metal contents of catalyst for oxygen reduction.

Numerous studies have been carried out using Nb<sub>x</sub>Ti<sub>(1-x)</sub>O<sub>2</sub> and have reported high activity and stability. The synthesized in Ref. [37] 20 wt.% Pt/Nb<sub>0.05</sub>Ti<sub>0.95</sub>O<sub>2</sub> catalyst, in comparison with Vulcan supported one, showed similar catalytic activity towards oxygen reduction, expressed through the specific current densities at the constant potential, especially in the potential range of practical interest (0.85-0.90 V vs. RHE). Although the catalytic activities are similar, the

importance of new synthesized  $\text{Nb}_{0.05}\text{Ti}_{0.95}\text{O}_2$  support could be emphasized as it is proved to be more stable than carbon-based support in aqueous electrolytes.

A simple wet-chemical route to grow Pt nanoparticles on mesoporous Nb-TiO<sub>2</sub> hollow spheres with controlled Pt loadings in environmentally friendly aqueous solution was presented in Ref. [38]. These Pt/Nb-TiO<sub>2</sub> catalysts exhibit higher catalytic activity for ORR and better stability than the benchmark E-TEK commercial Pt/C catalysts.

It has been demonstrated [39] that Pt supported on Nb-doped TiO<sub>2</sub> nanofibers (Nb: 10 mol%) was much more stable than reduced or calcined Pt/TiO<sub>2</sub> catalysts and the commercially available Pt/C when subjected to 1000 voltammetric cycles in the range of 0.05-1.3 V.

### **1.3 Application of NiWO<sub>4</sub>-based composite supported Pt catalysts as anode and cathode in PEM fuel cell**

Design and preparation of mesoporous nickel-tungsten mixed oxides and their composite with different carbonaceous materials can be also a promising direction in the development of bifunctional anode and cathode Pt electrocatalysts. In this respect, the choice of NiWO<sub>4</sub>, which are stable in an acidic media and have good proton conductivity, seems to be quite promising. NiWO<sub>4</sub> nanoparticles and their composites exhibit interesting electrochemical properties, for example, in oxygen evolution reactions [40], electrocatalytic conversion of N<sub>2</sub> to NH<sub>3</sub> [41], etc. Moreover, Pt/NiWO<sub>4</sub> system has been patented as anode electrocatalysts for alcohol oxidation [42]: it has been supposed that in aqueous solutions the NiWO<sub>4</sub> support removes the carbon monoxide intermediates by creating OH species at the outer surface. Considerable improvement of the ORR activity in an alkaline medium was achieved after loading of 10 wt.% of Pt on a NiWO<sub>x</sub> solid solution with plenty of oxygen defects prepared by the displacement of Ni in the W<sub>18</sub>O<sub>49</sub> lattice [43].

However, the mixed oxide NiWO<sub>4</sub> has a relative low electrical conductivity and a low specific surface area, which is a disadvantage when used as a support for electrocatalysts. New types of carbonaceous materials like, carbon nanotubes, reduced graphene oxides (rGOs) have also been reported to provide extreme good properties to metal oxide-carbonaceous composites due to their special electronic structure [44].

The aim of this work was to study the effect of composition and structure of corrosion resistant mixed oxide-based cathode and anode electrocatalysts on the activity in the ORR and HOR in acidic medium. The key element of the concept was the introduction of composite

support materials containing metal oxides to replace the carbon support in the corrosion-sensitive Pt/C electrocatalysts.

In the present report, the activity both in HOR and ORR of the Pt/Ti<sub>(1-x)</sub>M<sub>x</sub>O<sub>2</sub>-C (M: Mo, Nb) catalytic systems developed by the RERG was investigated. Based on our preliminary studies, the most promising catalysts prepared with different oxide/carbon ratios and different types of carbon backbones were selected for a detailed electrochemical study.

Additionally, the Ni-based nanoarchitected NiWO<sub>4</sub>-GNP (GNPs: graphene nanoplatelets) support material provided by Romanian colleagues in the frame of cooperation with the “Ilie Murgulescu” Institute of Physical Chemistry of the Romanian Academy, have been investigated as well. Composite NiWO<sub>4</sub>-GNP was loaded with 40 wt.% Pt via a modified NaBH<sub>4</sub>-assisted ethylene-glycol reduction-precipitation method developed in the RERG and the prepared catalyst was tested in both electrocatalytic reactions.

## 2. Experimental

### 2.1. Electrocatalysts used

According to our preliminary studies, six the most promising catalysts for use as anode and cathode in PEM fuel cells were selected for detailed electrochemical study.

Throughout this report the Ti<sub>(1-x)</sub>M<sub>x</sub>O<sub>2</sub>-C (M: Mo, Nb) composites will be identified by the nominal oxide/carbon mass ratio, along with the type of carbon used (C: Vulcan (**V**), unmodified (**BP**) and functionalized Black Pearls 2000 (**F-BP**): e.g., 25Ti<sub>(1-x)</sub>M<sub>x</sub>O<sub>2</sub>-75V means the composite of 25 wt.% of mixed oxide and 75 wt.% of Vulcan carbon.

#### *Preparation and characterization of anode electrocatalysts*

In our previous study [22] an optimized route for preparation of Ti<sub>0.8</sub>Mo<sub>0.2</sub>O<sub>2</sub>-C composite supports for Pt electrocatalysts with 25/75 oxide/carbon mass ratio containing mixed oxide with Ti/Mo atomic ratio of 80/20 (Ti<sub>0.8</sub>Mo<sub>0.2</sub>O<sub>2</sub>) was elaborated. The functionalization of carbon is carried out as follows: commercial BP carbon previously pre-treated in nitrogen at 1000 °C was modified using a two-step treatment with HNO<sub>3</sub> and glucose (F-BP) (details of such treatments are given in the Ref. [19]). The structural and compositional properties of the composite materials and related Pt catalysts were explored by transmission electron microscopy, X-ray diffraction and N<sub>2</sub> adsorption measurements. Properties of the three anode electrocatalysts with nominal composition 20 wt.% Pt/25Ti<sub>0.8</sub>Mo<sub>0.2</sub>O<sub>2</sub>-75C (C: **V**, unmodified **BP** and functionalized

**F-BP**) are summarized in Table 1. Electrochemical experiments presented in this report were used to assess the functional properties of the catalysts.

**Table 1.** Characterization of the  $\text{Ti}_{0.8}\text{Mo}_{0.2}\text{O}_2\text{-C}$  composites and the related Pt catalysts by TEM, XRD and nitrogen adsorption measurements [22].

Catalyst <sup>a)</sup>	$S_{\text{BET}}$ <sup>b)</sup> ( $\text{m}^2/\text{g}$ )	Pt size, nm (TEM)	Lattice parameters, $\text{\AA}$ <sup>c)</sup>	Mo subst., %
20 wt.% Pt/25 $\text{Ti}_{0.8}\text{Mo}_{0.2}\text{O}_2\text{-75BP}$	1120	$2.7 \pm 0.7$	$a= 4.630, c= 2.940$	18
20 wt.% Pt/25 $\text{Ti}_{0.8}\text{Mo}_{0.2}\text{O}_2\text{-75F-BP}$	726	$2.8 \pm 0.7$	$a= 4.630, c= 2.940$	18
20 wt.% Pt/25 $\text{Ti}_{0.8}\text{Mo}_{0.2}\text{O}_2\text{-75V}$	175	$2.0 \pm 0.6$	$a= 4.630, c= 2.940$	18

<sup>a)</sup> **BP**: Black Pearls 2000; **F-BP**: BP carbon pre-treated at 1000°C in nitrogen for 3 h before functionalization, then functionalized with  $\text{HNO}_3$  and glucose; **V**: Vulcan.

<sup>b)</sup> Specific surface area of the composite support materials determined by nitrogen adsorption measurements;

<sup>c)</sup> Lattice parameters of the rutile phase obtained after high-temperature treatment; pure rutile  $\text{TiO}_2$ :  $a= 4.593 \text{ \AA}$ ,  $c= 2.959 \text{ \AA}$ .

#### *Preparation and characterization of cathode electrocatalysts*

Properties and preparation details of the 40 wt.% Pt cathode electrocatalysts are summarized in Table 2.

**Table 2.** Properties and preparation details of the composites used as a support for 40 wt.% Pt cathode electrocatalysts

Catalyst	$S_{\text{BET}}$ ( $\text{m}^2/\text{g}$ )	Preparation details
Pt/75 $\text{Ti}_{0.93}\text{Nb}_{0.07}\text{O}_2\text{-25BP}$	273	The composite was prepared using a synthesis route developed for samples with high oxide content (details see in Ref. [22])
Pt/25 $\text{Ti}_{0.93}\text{Nb}_{0.07}\text{O}_2\text{-75V}$	n.d.	The composite was prepared using a synthesis route developed for samples with high carbon content (details see in Ref. [22])
Pt/ $\text{NiWO}_4\text{-GNP}$	29	$\text{NiWO}_4$ materials with Ni/W= 1:1 ratio were synthesized by co-precipitation of Ni and W precursor compounds using EG as template and TBAOH as pH mediator; composites with rGO were prepared using direct synthesis method

n.d., no data

Our research group has recently developed the synthesis of novel  $\text{Ti}_{0.93}\text{Nb}_{0.07}\text{O}_2\text{-C}$  (C: BP, V; oxide/carbon ratios: 75/25 and 25/75) composite supports for Pt electrocatalysts using ammonium niobate (V) oxalate hydrate as Nb precursor compound. Upon the preparation of  $\text{Ti}_{0.93}\text{Nb}_{0.07}\text{O}_2\text{-C}$  composites the success of the sol-gel-based multistep synthesis followed by high-temperature treatment (HTT: Ar, 600 °C, 8 h) was usually controlled by XRD, in which incorporation of Nb is detected as a characteristic distortion of the  $\text{TiO}_2$ -rutile unit cell. In previous studies of the RERG, it has been demonstrated that exclusive incorporation of Nb in the  $\text{TiO}_2$  is feasible only up to a certain solubility limit (below 10 atomic% Nb), above which segregated ionic Nb species remained on the surface. Details of the preparation of Nb-containing composite materials with different  $\text{Ti}_{0.93}\text{Nb}_{0.07}\text{O}_2\text{/C}$  ratios (C: BP, Vulcan) were presented in Table 3.

**Table 3.** Nominal composition and preparation details of the Nb-containing composites with the different  $\text{Ti}_{0.93}\text{Nb}_{0.07}\text{O}_2\text{/C}$  ratios (C: BP, Vulcan)

Samples nominal composition <sup>a)</sup>	TiO <sub>2</sub> sol			Suspension of carbon			Nb prec. <sup>b)</sup> (g)
	H <sub>2</sub> O (ml)	HNO <sub>3</sub> (ml)	Ti prec. <sup>b)</sup> (ml)	Carbon (g)	H <sub>2</sub> O (ml)	HNO <sub>3</sub> <sup>c)</sup> (ml)	
75Ti <sub>0.93</sub> Nb <sub>0.07</sub> O <sub>2</sub> -25BP	25.4	2.85	2.487	0.25	10	-	0.1915
25Ti <sub>0.93</sub> Nb <sub>0.07</sub> O <sub>2</sub> -75V	8.46	0.95	0.83	0.75	15	0.78	0.0638

<sup>a)</sup> Expected composition of composites with different  $\text{Ti}_{0.93}\text{Nb}_{0.07}\text{O}_2\text{/C}$  mass ratio;

<sup>b)</sup> Ti and Nb precursor compounds:  $(\text{Ti}(\text{O}-i\text{-Pr})_4$  and  $(\text{NH}_4)\text{NbO}(\text{C}_2\text{O}_4)_2 \times \text{H}_2\text{O}$ );

<sup>c)</sup> cc. HNO<sub>3</sub> (65%, Molar Chemicals, a.r.).

Composite of mesoporous  $\text{NiWO}_4$  with graphene nanoplatelets (10 wt.%), for use as bifunctional cathode electrocatalyst, was synthesized by Romanian colleagues using a facile co-precipitation synthesis route (see Table 2). Inexpensive and commercially available GNPs (with a surface area of 300 m<sup>2</sup>/g, Sigma-Aldrich), which are hybrids between graphene and graphite, were used as carbonaceous material to increase both the conductivity and surface area of the catalyst.

## 2.2. Preparation of the 20 and 40 wt.% Pt electrocatalysts

Composite support materials were loaded with 20 and 40 wt.% Pt via a modified  $\text{NaBH}_4$ -assisted ethylene-glycol (EG) reduction-precipitation method demonstrated schematically in Figure 1 [15]. The flowchart of this process can be seen in Figure 1 (for more details see Table 1).

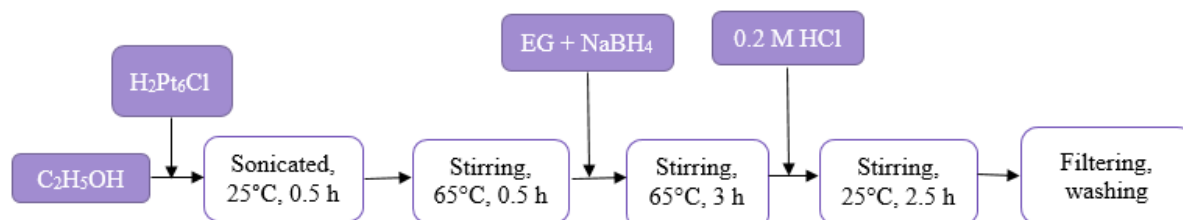


**Figure 1.** Flow chart for synthesis of 20 and 40 wt.% Pt electrocatalysts

As a first step of preparation procedure,  $\text{H}_2\text{PtCl}_6 \times 6\text{H}_2\text{O}$  was dissolved in ethanol in a round bottom flask. The 200 mg of the support material was dispersed in the solution by sonication at room temperature and the suspension was heated up to 65 °C with continuous stirring. A solution prepared by mixing of  $\text{NaBH}_4$  and EG was added dropwise to the suspension very slowly and carefully with a syringe pump in 30 minutes at 65 °C with continuous stirring. After the addition of 30 minutes the system was stirred at 65 °C for 3 hours. Hydrogen chloride solution was added to the suspension and it was stirred for an additional 2.5 hours at room temperature in order to allow the Pt particles to settle on the surface of the support. The materials were washed four times with 50 ml water and filtered by centrifugation in order to remove the chloride ions and dried at 85 °C in an oven overnight.

**Table 4.** Preparation details of the 20 and 40 wt.% Pt electrocatalysts

Pt content	$\text{H}_2\text{PtCl}_6 \times 6\text{H}_2\text{O}$ , mg	abs. EtOH, ml	$\text{NaBH}_4$ solution in EG			0.2 M HCl, ml
			$\text{NaBH}_4$ , mg	EG, ml	added ( $\text{NaBH}_4$ + EG) solution, ml	
20 wt.% Pt	134	50	596	7.4	3.7	15
40 wt.% Pt	353.9	50	805.4	10	7.4	30

## **2.3. Electrochemical characterization**

### **2.3.1. Electrochemical characterization by cyclic voltammetry**

All electrocatalysts were investigated by means of cyclic voltammetry (CV) in a conventional three-electrode electrochemical glass cell using a Biologic SP150 potentiostat and the EC-LAB software package. The working electrode was prepared by supporting the electrocatalysts on a glassy carbon (GC) electrode ( $d = 0.3$  cm, geometric surface area  $A = 0.0707$  cm<sup>2</sup>).

The electrode was polished by means of alumina powder (10  $\mu$ m diameter) with the addition of isopropanol in order to remove the impurities from the surface. Subsequently, the polishing alumina powder was removed from the electrode surface by rinsing with distilled water. The sample to be examined was powdered and an ink was prepared by dispersing 2 mg of the catalyst samples in 2 ml of a mixture of 1.592 ml of MilliQ water, 0.4 ml of isopropanol and 8  $\mu$ l of 5% Nafion<sup>®</sup> solution (DuPont<sup>™</sup> Nafion<sup>®</sup> PFSA Polymer Dispersions DE 520). The suspension was sonicated for 30 minutes. From this suspension a drop (3.6  $\mu$ l) was pipetted on to the dry mirror-polished GC and dried at room temperature for 20 min.

The reference electrode was a hydrogen electrode immersed in the same electrolyte as the working electrode and all potentials are given on the RHE scale. Pt was used as counter electrode. All electrochemical measurements were carried out at ambient temperature. Solutions were prepared from Millipore MilliQ water and P.A. reagents. 5.5 N Ar gas was used for deoxygenation the solutions. The electrolyte was 0.5 M H<sub>2</sub>SO<sub>4</sub> (Merck).

Prior to the measurements, the electrode was activated by potential cycling for 10 times in the range 50 and 1000 mV at a scan rate of 100 mV s<sup>-1</sup>. After the activation procedure, CV measurements were done in the potential range of 50-1000 mV at a scan rate of 10 mV s<sup>-1</sup>.

For comparison activity in the HOR and ORR commercially available reference 20 and 40 wt.% Pt/C (Quintech, C-20-Pt and C-40-Pt on Vulcan; denoted hereafter as 20Pt/C and 40Pt/C, respectively) electrocatalysts were also studied by the same methods as described above.

### **2.3.2. Electrochemical characterization by ORR**

Catalytic activity of the catalyst samples was tested in the ORR by rotating disc electrode (RDE) technique. A RDE is a hydrodynamic working electrode used in a three-electrode system. The electrode rotates during experiments inducing the diffusion of reactant to the electrode via a well-defined stationary electrolyte layer, the thickness of which depends on the rotational speed.

The rotating speed of the electrode can be controlled at different levels, which yields a different diffusion rate of the reactant.

The ORR measurements were done in O<sub>2</sub> saturated 0.5 M H<sub>2</sub>SO<sub>4</sub> solution. The diameter of GC electrode and Pt loading used in these experiments was the same as during CV measurements. Polarization curves were recorded by cathodic scan sweeping the potential between 1000 and 200 mV with 10 mVs<sup>-1</sup> sweep rate, rotating the electrode at 225, 400, 625, 900, 1225 and 1600 revolutions/min (rpm). In order to characterize the surface state of the catalysts, before and after the RDE measurements 10 CVs between 50 and 1000 mV potential window in Ar saturated electrolyte were also measured.

### 2.3.3. Electrochemical characterization by HOR

Catalytic activity in the hydrogen oxidation reaction was also investigated by RDE method in hydrogen saturated 0.5 M H<sub>2</sub>SO<sub>4</sub> solution at 400, 625, 900, 1225 and 1600 rpm. Polarization curves were recorded by anodic scan sweeping the potential between 0 and 300 mV with 10 mVs<sup>-1</sup> sweep rate. The diameter of GC electrode and Pt loading used in these experiments was the same as during CV and ORR measurements.

## 3. Results and discussion

### 3.1. Electrochemical characterization of the Pt/Ti<sub>0.8</sub>Mo<sub>0.2</sub>O<sub>2</sub>-C anode electrocatalysts

In order to clarify the possibility of using novel 20 wt.%Pt/Ti<sub>0.8</sub>Mo<sub>0.2</sub>O<sub>2</sub>-C catalysts (C: V, BP and F-BP, Ti<sub>0.8</sub>Mo<sub>0.2</sub>O<sub>2</sub>/C: 25/75) as anode or cathode in PEM fuel cells, their electrochemical characteristics were investigated. The influence of the type of carbonaceous materials on the performance in the ORR and the HOR expressed as current values normalized to the geometric surface area of the electrode was compared on Figure 2. Comparable values of the electrochemically active Pt surface area (ECSA) calculated from the charge of the hydrogen desorption were obtained for all composite supported electrocatalysts (see Table 5).

**Table 5.** Electrochemical performance of the Ti<sub>0.8</sub>Mo<sub>0.2</sub>O<sub>2</sub>-C composite supported 20 wt.% Pt electrocatalysts

Catalyst	Nominal composition	CV	ECSA, m <sup>2</sup> /g <sub>Pt</sub>	ORR	HOR
Pt/75BP	Pt/25Ti <sub>0.8</sub> Mo <sub>0.2</sub> O <sub>2</sub> -75BP	+	69.9 ± 3.2	+	+
Pt/75F-BP	Pt/25Ti <sub>0.8</sub> Mo <sub>0.2</sub> O <sub>2</sub> -75F-BP	+	68.1 ± 2.4	+	+
Pt/75V	Pt/25Ti <sub>0.8</sub> Mo <sub>0.2</sub> O <sub>2</sub> -75V	+	70.3 ± 3.4	+	+
Pt/C	Pt/C	+	94.5 ± 2.5	+	+

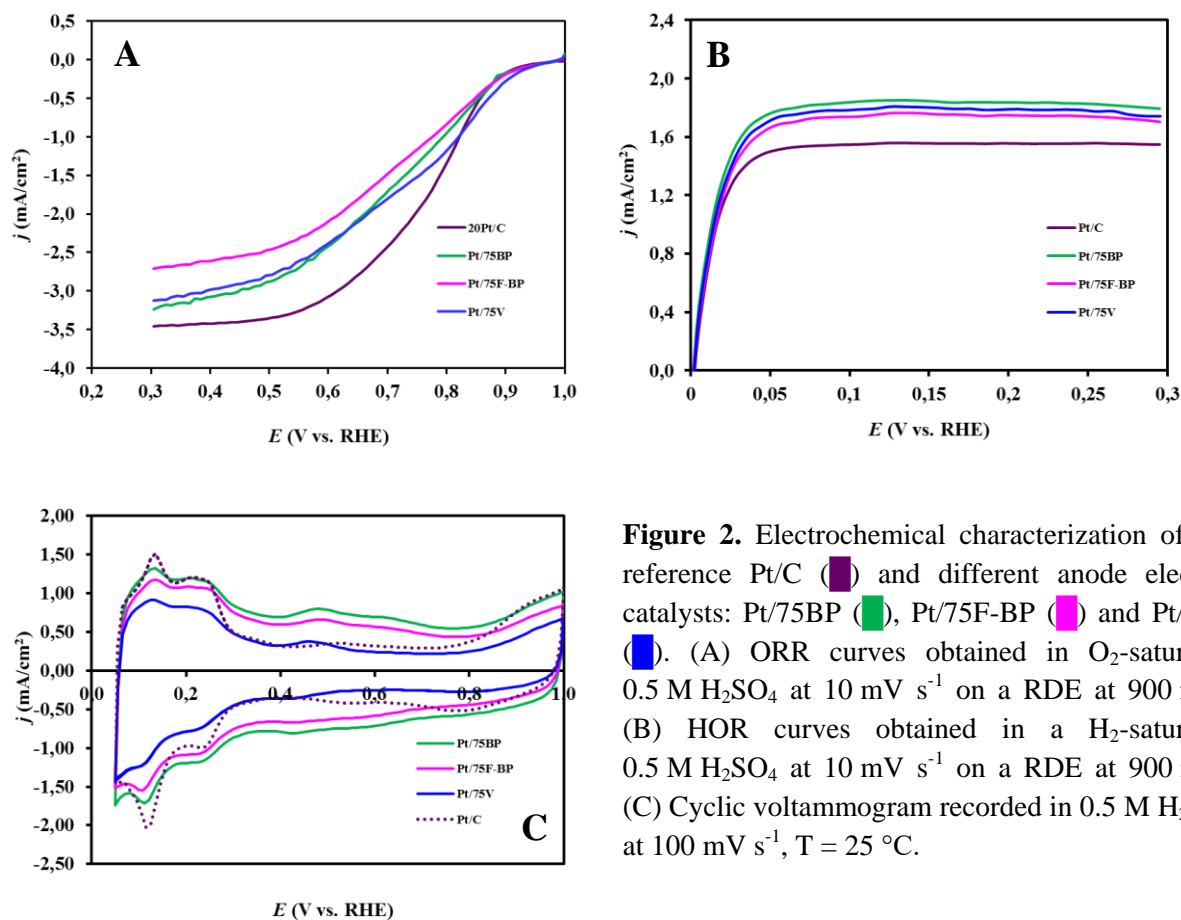


**Figure 2.** Electrochemical characterization of the reference Pt/C (■) and different anode electrocatalysts: Pt/75BP (■), Pt/75F-BP (■) and Pt/75V (■). (A) ORR curves obtained in O<sub>2</sub>-saturated 0.5 M H<sub>2</sub>SO<sub>4</sub> at 10 mV s<sup>-1</sup> on a RDE at 900 rpm; (B) HOR curves obtained in a H<sub>2</sub>-saturated 0.5 M H<sub>2</sub>SO<sub>4</sub> at 10 mV s<sup>-1</sup> on a RDE at 900 rpm. (C) Cyclic voltammogram recorded in 0.5 M H<sub>2</sub>SO<sub>4</sub> at 100 mV s<sup>-1</sup>, T = 25 °C.

Catalytic activity after 10 cycles of conditioning of the commercial reference 20 wt.% Pt/C and composite supported Pt catalysts was investigated in the ORR by RDE technique in O<sub>2</sub> saturated 0.5 M H<sub>2</sub>SO<sub>4</sub> solution (see Figure 2.A). Potential dynamic polarization curves obtained on RDE at six rotation speeds (225, 400, 625, 900, 1225 and 1600 rpm) for all catalysts were demonstrated on Figure 3.

As shown in Fig. 2.A, current density of the ORR in the mixed kinetic-diffusion controlled region on the fresh reference Pt/C catalyst was higher comparing to the composite supported Pt catalysts. Identical diffusion limited currents were reached on the Pt/75BP and Pt/75V catalysts, whereas the limiting current of the Pt/75F-BP catalyst was slightly lower.

Figure 2.B displays HOR voltammograms (positive-going scans) recorded via the rotating disc electrode technique in H<sub>2</sub>-saturated 0.5 M H<sub>2</sub>SO<sub>4</sub> ( $v = 10 \text{ mV s}^{-1}$ , T = 25 °C and  $\omega = 900 \text{ rpm}$ ) on the Pt/C and different carbonaceous materials-containing Pt/Ti<sub>0.8</sub>Mo<sub>0.2</sub>O<sub>2</sub>-C electrocatalysts. The currents were also normalized to the geometric area of the glassy carbon electrode.

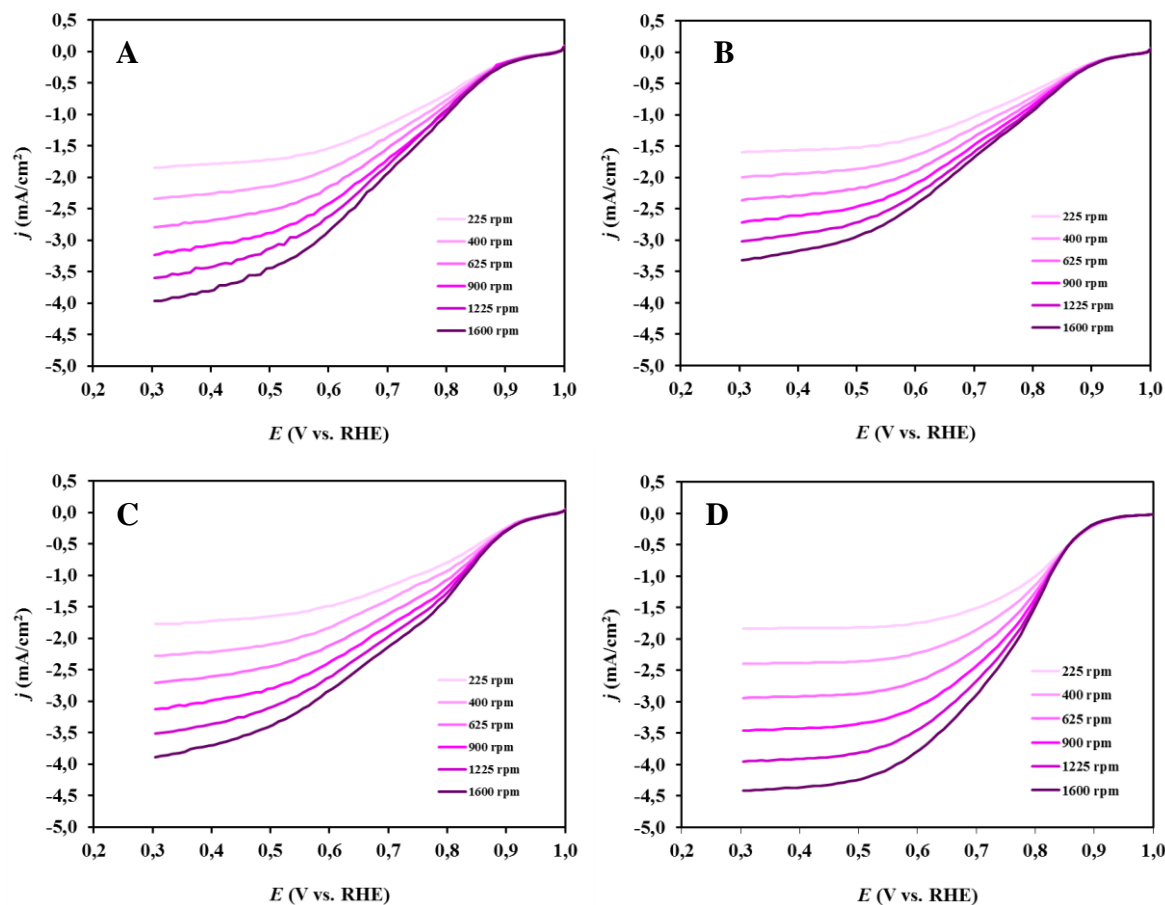


**Figure 3.** Potentiodynamic ( $10 \text{ mV s}^{-1}$ , negative sweep) oxygen reduction current densities obtained in O<sub>2</sub>-saturated 0.5 M H<sub>2</sub>SO<sub>4</sub> at 225, 400, 625, 900, 1225 and 1600 rpm: (A) 20 wt.% Pt/25Ti<sub>0.8</sub>Mo<sub>0.2</sub>O<sub>2</sub>-75BP, (B) 20 wt.% Pt/25Ti<sub>0.8</sub>Mo<sub>0.2</sub>O<sub>2</sub>-75F-BP, (C) 20 wt.% Pt/25Ti<sub>0.8</sub>Mo<sub>0.2</sub>O<sub>2</sub>-75V, and (D) 20 wt.% Pt/C Quintech electrocatalyst.

It can be seen from Figure 2.B that the electrochemical performance of Pt/Ti<sub>0.8</sub>Mo<sub>0.2</sub>O<sub>2</sub>-C electrocatalysts was nearly identical, while the reference 20 wt.% Pt/C catalyst shows a slightly lower HOR current. The limiting current density of the Pt/C catalyst is only slightly lower than that of composite supported Pt electrocatalysts. Potential dynamic polarization curves obtained on RDE at five rotation speeds (400, 625, 900, 1225 and 1600 rpm) for all catalysts were demonstrated on Figure 4.

It is well known that the rate of the oxidation of hydrogen on the Pt electrode in acid solution might be too fast to be measured with the RDE method [45] [46] [47]. On the polarization curves for HOR obtained in RDE measurements at room temperatures, the steady-state current generally

risers sharply from the origin with positive going potential and reaches a limiting plateau above 50 mV.

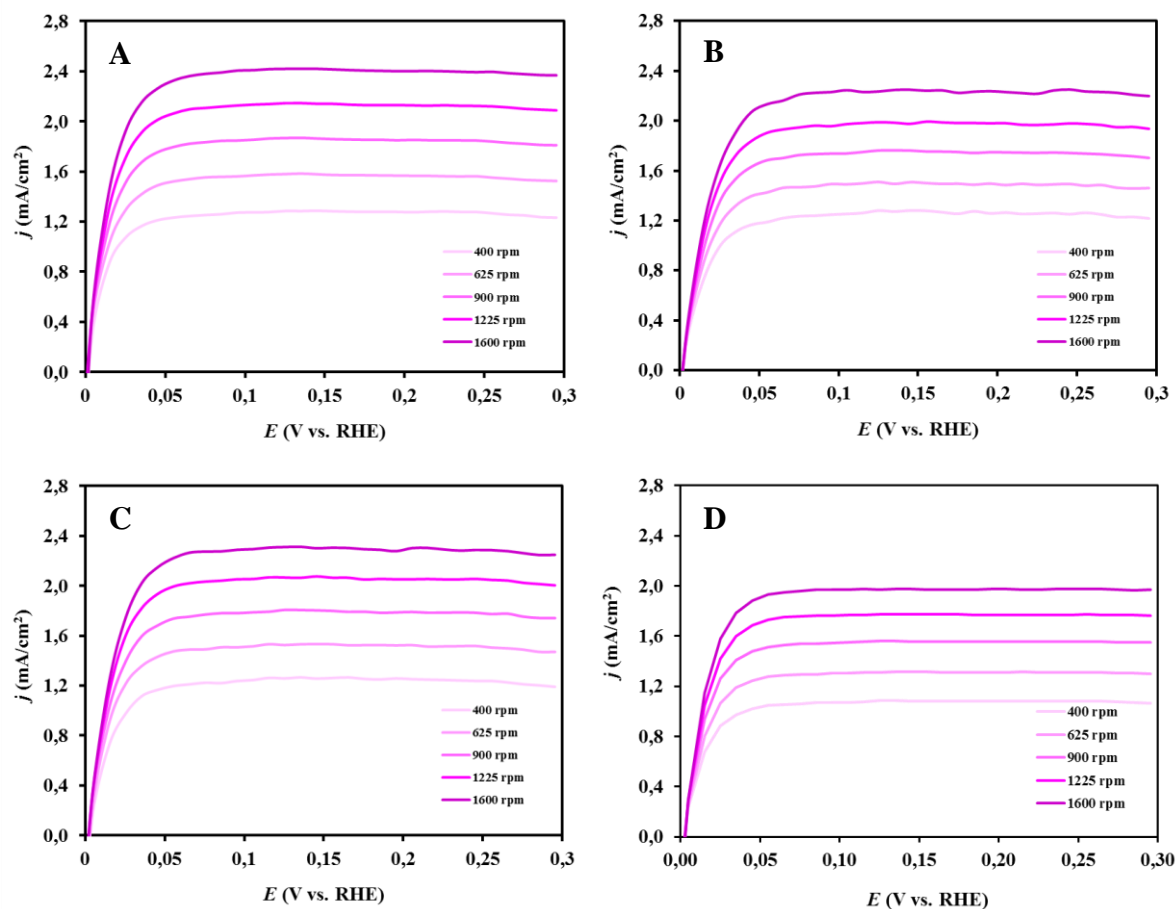


**Figure 4.** Potentiodynamic hydrogen oxidation current densities obtained in H<sub>2</sub>-saturated 0.5 M H<sub>2</sub>SO<sub>4</sub> at 400, 625, 900, 1225 and 1600 rpm: (A) 20 wt.% Pt/25Ti<sub>0.8</sub>Mo<sub>0.2</sub>O<sub>2</sub>-75BP, (B) 20 wt.% Pt/25Ti<sub>0.8</sub>Mo<sub>0.2</sub>O<sub>2</sub>-75F-BP, (C) 20 wt.% Pt/25Ti<sub>0.8</sub>Mo<sub>0.2</sub>O<sub>2</sub>-75V, and (D) 20 wt.% Pt/C Quintech electrocatalyst. Sweep rate: 10 mV s<sup>-1</sup>.

A typical cyclic voltammogram of Pt with the classical features of the adsorption/desorption of underpotentially deposited hydrogen between 50 and 350 mV along with a redox peak pair of the Mo between 380 and 530 mV was observed on the all studied catalysts (see Figure 2.C). According to the literature and our previous results [18] [48] [49] the appearance of these redox peaks in the voltammograms clearly confirm that there is an active interface between the Pt nanoparticles and the surface Mo species of the composite support. It should be noted, that, as shown in Figure 2.C, the charge of the double layer depends on the type of carbonaceous

materials used for the preparation of the catalysts and correlates well with the BET surface area of the composite materials calculated on the basis  $N_2$  adsorption measurements (see Table 1).

### 3.2. Electrochemical characterization of mixed oxide-containing cathode catalysts

A comparison of the electrocatalytic behavior of 40 wt.% Pt catalysts in a standard three-electrode cell was presented in Figure 5.

**Table 6.** Electrochemical performance of mixed oxide-containing cathode 40 wt.% Pt electrocatalysts

Catalyst <sup>a)</sup>	CV	ECSA, $m^2/g_{Pt}$	ORR	HOR
Pt/75Ti <sub>0.93</sub> Nb <sub>0.07</sub> O <sub>2</sub> -25BP	+	49.7 ± 2.7	+	+
Pt/25Ti <sub>0.93</sub> Nb <sub>0.07</sub> O <sub>2</sub> -75V	+	50.4 ± 1.2	+	+
Pt/NiWO <sub>4</sub> -GNP	+	65.3 ± 2.0	+	+
Pt/C	+	44.3 ± 3.1	+	+

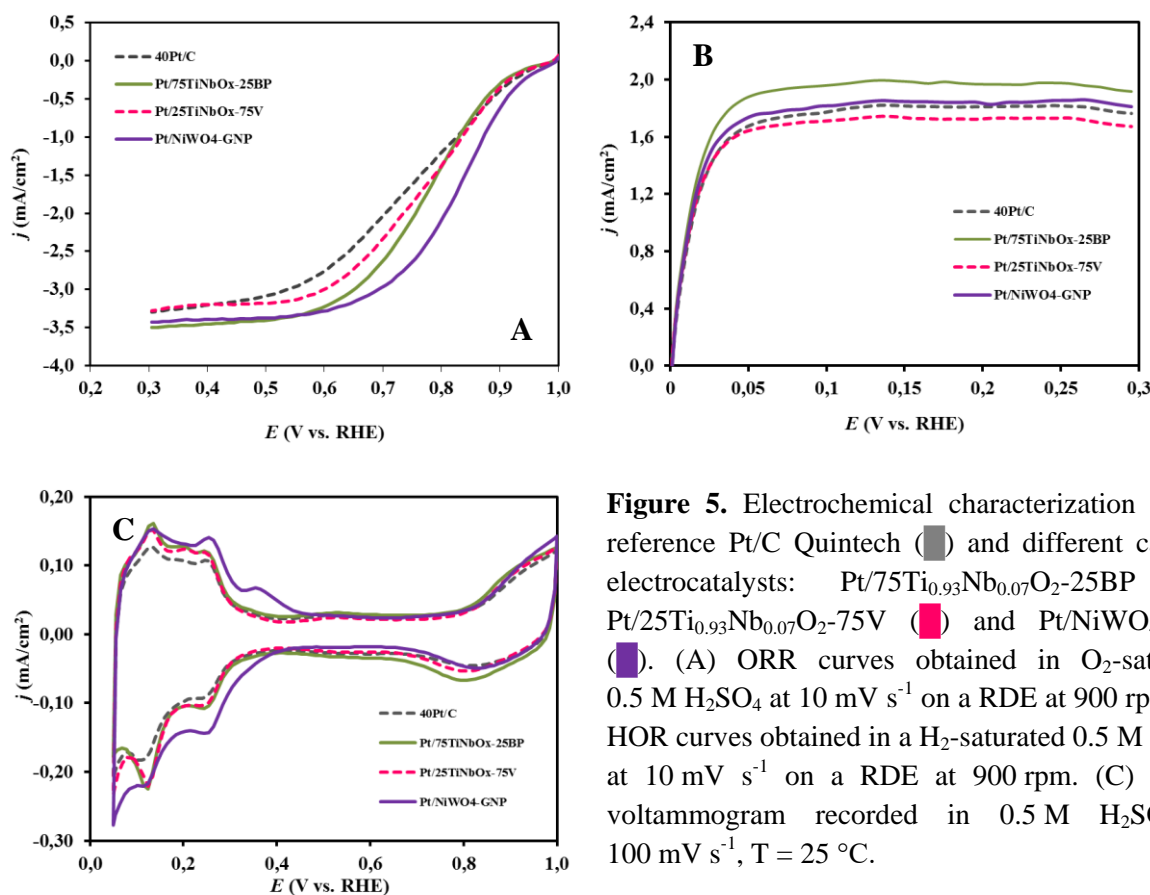


**Figure 5.** Electrochemical characterization of the reference Pt/C Quintech (■) and different cathode electrocatalysts: Pt/75Ti<sub>0.93</sub>Nb<sub>0.07</sub>O<sub>2</sub>-25BP (■), Pt/25Ti<sub>0.93</sub>Nb<sub>0.07</sub>O<sub>2</sub>-75V (■) and Pt/NiWO<sub>4</sub>-GNP (■). (A) ORR curves obtained in O<sub>2</sub>-saturated 0.5 M H<sub>2</sub>SO<sub>4</sub> at 10 mV s<sup>-1</sup> on a RDE at 900 rpm; (B) HOR curves obtained in a H<sub>2</sub>-saturated 0.5 M H<sub>2</sub>SO<sub>4</sub> at 10 mV s<sup>-1</sup> on a RDE at 900 rpm. (C) Cyclic voltammogram recorded in 0.5 M H<sub>2</sub>SO<sub>4</sub> at 100 mV s<sup>-1</sup>, T = 25 °C.

Potential dynamic polarization oxygen reduction and hydrogen oxidation curves (not shown) were obtained for all catalysts on RDE at six and five rotation speeds, respectively. It should be noted that obtaining reproducible results in the study of 40 wt.% Pt electrocatalysts is a rather difficult task (all measurements were repeated at least four to six times until reproducible results are obtained). Reproducibility of the cyclic voltammetry, ORR and HOR measurements in a standard three-electrode cell were demonstrated on Figures 6-9.

As shown in Figure 5.A the onset potential of the ORR on the reference Pt/C and both Nb-containing catalysts was observed at slightly less positive potential comparing to the Pt/NiWO<sub>4</sub>-GNP, indicating that these catalysts are less active. Moreover, the mixed kinetics-diffusion control region of the NiWO<sub>4</sub>-based catalyst is in the range from 0.6 V and 1.0 V, demonstrating that this catalyst performs well in the ORR. It can be seen from Figure 5.B that the electrochemical performance of all mixed oxide-containing electrocatalysts in the HOR was very similar, while the Pt/75Ti<sub>0.93</sub>Nb<sub>0.07</sub>O<sub>2</sub>-25BP catalyst shows a slightly higher activity.

As shown in Figure 5.C all catalysts studied show a typical CV of Pt with the classical features of the underpotentially deposited hydrogen desorption between 50 < E < 400 mV. Moreover, a characteristic feature of the voltammogram obtained on the Pt/NiWO<sub>4</sub>-GNP is the asymmetry in the so-called hydrogen region: there is quite pronounced peak in the anodic branch of the voltammogram above 350 mV overlapping with the oxidation peak of the adsorbed hydrogen strongly bounded to the Pt surface. It is well known [14] [50] [51] [52] that this peak belongs to the oxidation of tungsten bronze formed due to the hydrogen spillover. Cathodic counterpart (i.e. the current peak of the formation of the tungsten bronze) of this anodic peak coincides with the hydrogen-adsorption peaks of the platinum.

As shown in Table 5, the highest ECSA value was obtained on the Pt/NiWO<sub>4</sub>-GNP catalyst. The ECSA values increase in the following order: Pt/C < Pt/75Ti<sub>0.93</sub>Nb<sub>0.07</sub>O<sub>2</sub>-25BP ≈ Pt/25Ti<sub>0.93</sub>Nb<sub>0.07</sub>O<sub>2</sub>-75V < Pt/NiWO<sub>4</sub>-GNP.

### **3.3 Electrochemical characterization of the scaled-up materials**

The scale of the preparation of the most promising supports for cathode and anode catalysts on a scale of up to 1 g was also carried out. When loading Pt by a NaBH<sub>4</sub>-assisted ethylene glycol reduction-precipitation method, the best results were obtained using 0.2 g of composite support. Thus, the appropriate amount of 20 and 40 wt.% Pt electrocatalyst (1 g) was obtained in four-five batches.

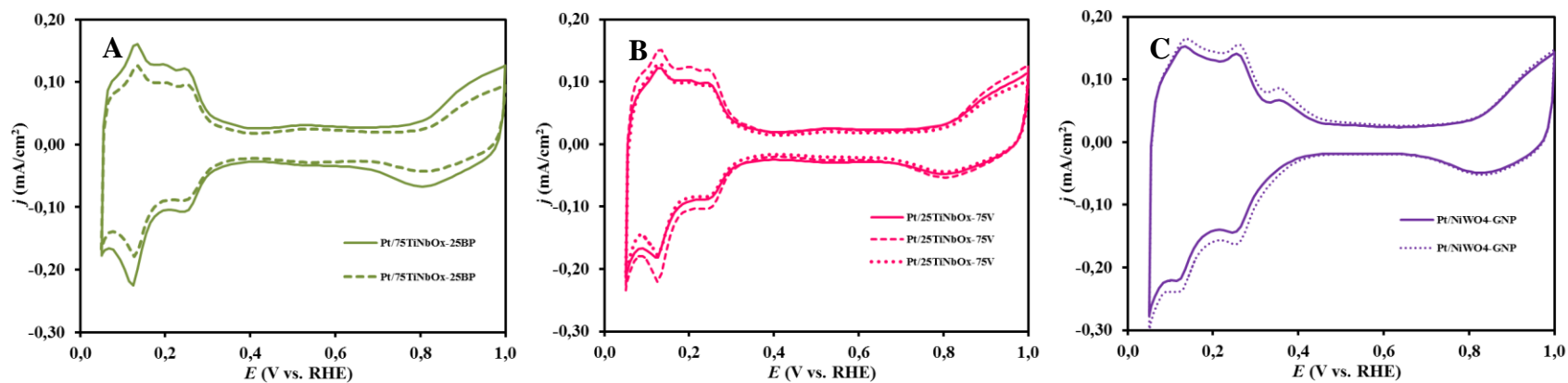


**Figure 6.** Reproducibility of the results obtained by cyclic voltammetry measurements on various Pt catalysts: (A) 40 wt.% Pt/75Ti<sub>0.93</sub>Nb<sub>0.07</sub>O<sub>2</sub>-25BP, (B) 40 wt.% Pt/25Ti<sub>0.93</sub>Nb<sub>0.07</sub>O<sub>2</sub>-75V and (C) 40 wt.% Pt/NiWO<sub>4</sub>-GNP.

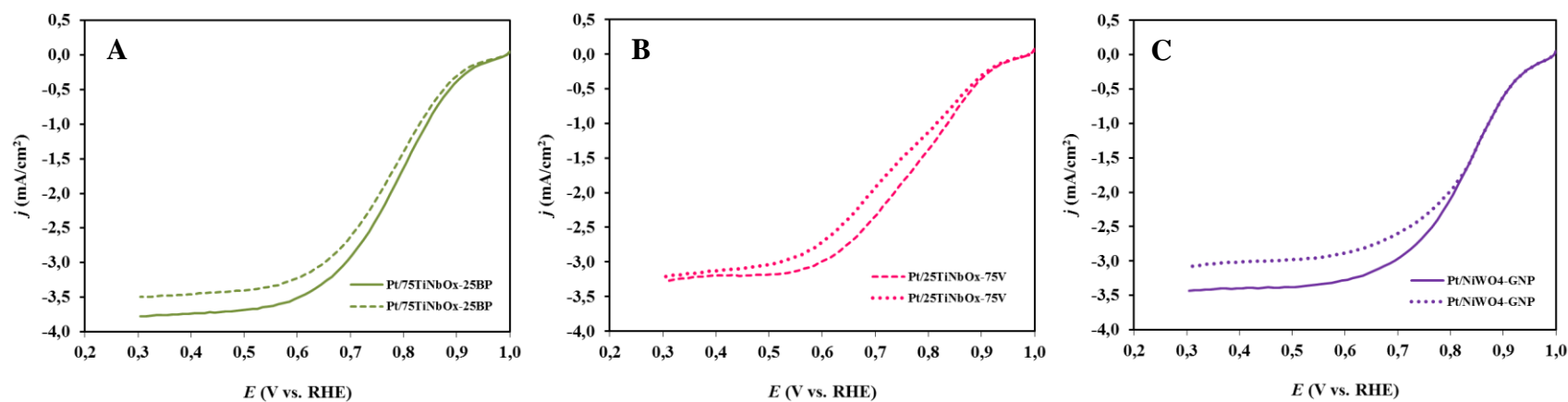


**Figure 7.** Reproducibility of the oxygen reduction reaction results obtained by RDE measurements on various Pt catalysts: (A) 40 wt.% Pt/75Ti<sub>0.93</sub>Nb<sub>0.07</sub>O<sub>2</sub>-25BP, (B) 40 wt.% Pt/25Ti<sub>0.93</sub>Nb<sub>0.07</sub>O<sub>2</sub>-75V and (C) 40 wt.% Pt/NiWO<sub>4</sub>-GNP.

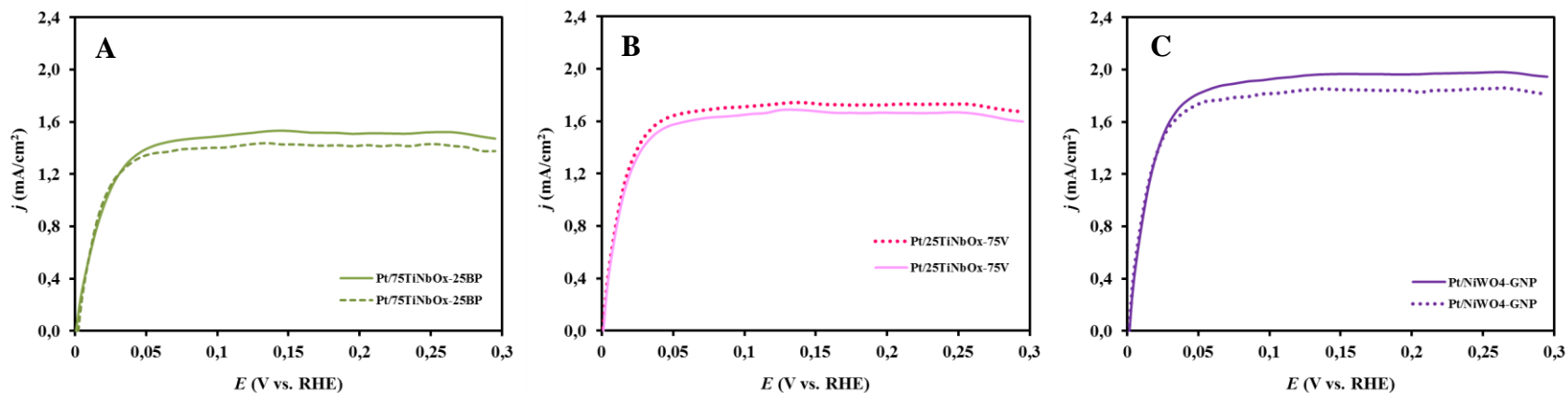


**Figure 8.** Reproducibility of the hydrogen oxidation reaction results obtained by RDE measurements on various Pt catalysts: (A) 40 wt.% Pt/75Ti<sub>0.93</sub>Nb<sub>0.07</sub>O<sub>2</sub>-25BP, (B) 40 wt.% Pt/25Ti<sub>0.93</sub>Nb<sub>0.07</sub>O<sub>2</sub>-75V and (C) 40 wt.% Pt/NiWO<sub>4</sub>-GNP.

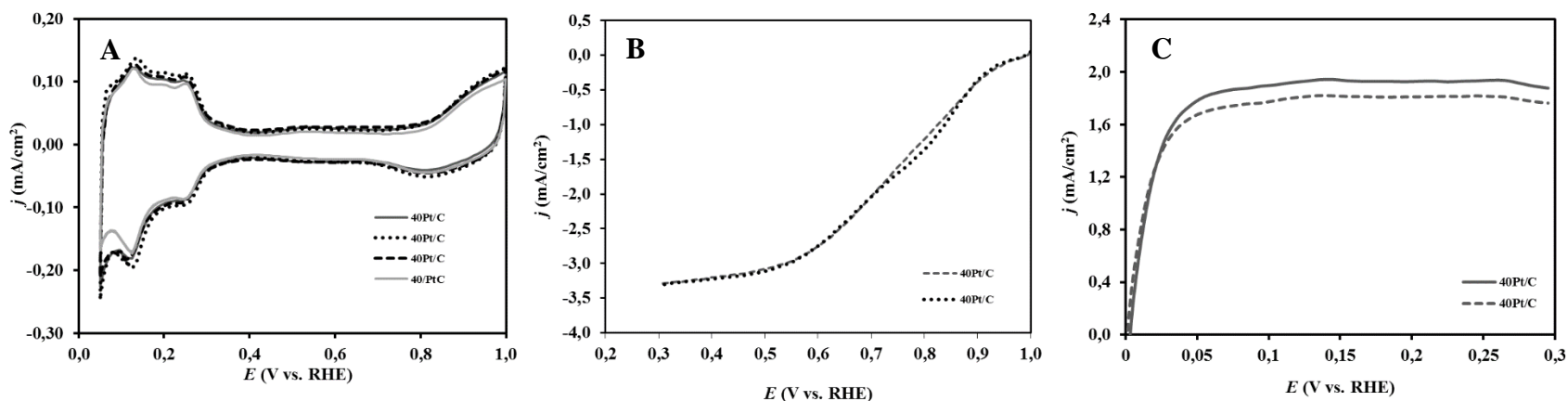


**Figure 9.** Electrochemical characterization of the reference Pt/C Quintech electrocatalyst: (A) Cyclic voltammogram recorded in 0.5 M H<sub>2</sub>SO<sub>4</sub> at 100 mV s<sup>-1</sup>, (B) ORR curves obtained in O<sub>2</sub>-saturated 0.5 M H<sub>2</sub>SO<sub>4</sub> at 10 mV s<sup>-1</sup> on a RDE at 900 rpm; (C) HOR curves obtained in a H<sub>2</sub>-saturated 0.5 M H<sub>2</sub>SO<sub>4</sub> at 10 mV s<sup>-1</sup> on a RDE at 900 rpm. T = 25 °C. Reproducibility of the RDE measurements results.

**Table 7.** Characterization of the scaled-up materials. Reproducibility of Pt loading

	20 wt.% Pt/25Ti <sub>0.8</sub> Mo <sub>0.2</sub> O <sub>2</sub> -75BP		40 wt.% Pt/75Ti <sub>0.93</sub> Nb <sub>0.07</sub> O <sub>2</sub> -25BP	
	1 <sup>st</sup> batch, 500 g	2 <sup>nd</sup> batch, 500 g	1 <sup>st</sup> batch, 500 g	2 <sup>nd</sup> batch, 500 g
<b>ECSA, m<sup>2</sup>/g<sub>Pt</sub></b>	69.9 ± 3.2	71.5±4.0	49.7±2.7	50.2±4.9

Characterization of different batches of Pt catalysts by cyclic voltammetry measurements was done before unifying them.

As shown in Figure 2.B, the 20 wt.% Pt/Ti<sub>0.8</sub>Mo<sub>0.2</sub>O<sub>2</sub>-C electrocatalysts exhibit very similar activity in the HOR. However, according to the results of the 10,000-cycle stability tests presented in our previous study [22] the Pt/25Ti<sub>0.8</sub>Mo<sub>0.2</sub>O<sub>2</sub>-75F-BP and Pt/25Ti<sub>0.8</sub>Mo<sub>0.2</sub>O<sub>2</sub>-75BP electrocatalysts have been selected as the most promising. Therefore, the scaling preparation procedure was carried out using 20 wt.% Pt/25Ti<sub>0.8</sub>Mo<sub>0.2</sub>O<sub>2</sub>-75BP catalyst as an anode.

In this series of experiments, the best activity in the ORR was obtained on the Pt catalyst supported on the composites of Ni-based materials with graphene nanoplatelets prepared using direct synthesis method (see Figure 5.A). However, preliminary results of our research group obtained using the catalysts presented in this report as the cathode for a PEM fuel cell showed that the performance of the Pt/NiWO<sub>4</sub>-GNP catalyst was worse in comparison with the optimal values. The activity of both Nb-containing catalysts was quite comparable. Thus, a catalyst with high Ti<sub>0.93</sub>Nb<sub>0.07</sub>O<sub>2</sub> mixed oxide content was selected for the scaling procedure.

As follows from Table 7, the results obtained on both electrocatalysts show good reproducibility of the synthesis.

#### 4. Summary

Based on our preliminary studies, the most promising Pt/Ti<sub>(1-x)</sub>M<sub>x</sub>O<sub>2</sub>-C (M: Mo, Nb) catalytic systems with different oxide/carbon ratios developed by the RERG, which were prepared using different types of carbon backbones, were studied in standard three-electrode cell. In addition, the activity of the 40 wt.% Pt/NiWO<sub>4</sub>-GNP catalyst in the ORR and HOR was also investigated.

According to the half-cell results TiO<sub>2</sub>-rutile-based 20 wt.% Pt/25Ti<sub>0.8</sub>Mo<sub>0.2</sub>O<sub>2</sub>-75C catalysts (Ti<sub>0.8</sub>Mo<sub>0.2</sub>O<sub>2</sub>/C: 25/75; C: Vulcan (V), unmodified (BP) and functionalized Black Pearls 2000 (F-BP)) can be recommended for use on the anode side of MEA in PEM fuel cell. Nevertheless, it should be noted, that the BP-based catalysts demonstrated better stability during 10,000-cycle long-term stability test.

According to the results obtained in the ORR by the RDE method, the activity of the 40 wt.% Pt/NiWO<sub>4</sub>-GNP catalyst was the highest. Although this electrocatalyst has shown promising ORR activity in half cell tests, the specific surface area of support does not reach the desired level, so further studies are needed. Probably the low surface is responsible for the inferior behavior in PEM fuel cell electrodes.

The preparation of promising cathode and anode catalysts on an enlarged scale has been carried out. The results obtained on both electrocatalysts show good reproducibility of the synthesis. In conclusion, electrochemical results presented in this report are a good starting point for further research.

## 5. References

- [1] C. Subban, Q. Zhou, A. Hu, T. E. Moylan, F. T. Wagner and F. J. DiSalvo, "Sol-Gel Synthesis, Electrochemical Characterization, and Stability Testing of Ti<sub>0.7</sub>W<sub>0.3</sub>O<sub>2</sub> Nanoparticles for Catalyst Support Applications in Proton-Exchange Membrane Fuel Cells," *J. Am. Chem. Soc.*, no. 132, pp. 17531-17536, 2010.
- [2] D. Wang, C. Subban, H. Wang, E. Rus, F. J. DiSalvo and H. Abruña, "Highly Stable and CO-Tolerant Pt/Ti<sub>0.7</sub>W<sub>0.3</sub>O<sub>2</sub> Electrocatalyst for Proton-Exchange Membrane Fuel Cells," *J. Am. Chem. Soc.*, no. 132, pp. 10218-10220, 2010.
- [3] V. T. T. Ho, C. J. Pan, J. Rick, W. N. Su and B. J. Hwang, "Nanostructured Ti<sub>0.7</sub>Mo<sub>0.3</sub>O<sub>2</sub> Support Enhances Electron Transfer to Pt: High-Performance Catalyst for Oxygen Reduction Reaction," *J. Am. Chem. Soc.*, no. 133, pp. 11716-11724, 2011.
- [4] T. Nguyen, V. Ho, C. J. Pan, J. Y. Liu, . H. Chou, J. Rick, . W. Su and B. J. Hwang, "Synthesis of Ti<sub>0.7</sub>Mo<sub>0.3</sub>O<sub>2</sub> supported- Pt nanodendrites and their catalytic activity and stability for oxygen reduction reaction," *Appl. Catal. B: Environ*, Vols. 183-189, no. 154-155, 2014.
- [5] K. Park and K. Seol, "Nb-TiO<sub>2</sub> supported Pt cathode catalyst for polymer electrolyte membrane fuel cells," *Electrochem Commun*, vol. 9, pp. 2256-2260, 2007.
- [6] S. Huang, P. Ganesan and B. N. Popov, "Electrocatalytic activity and stability of niobium-doped titanium oxide supported platinum catalyst for polymer electrolyte membrane fuel cells," *Appl Catal B: Environ*, no. 96, pp. 224-231, 2010.

- [7] A. Kumar and V. Ramani, "Ta<sub>0.3</sub>Ti<sub>0.7</sub>O<sub>2</sub> Electrocatalyst Supports Exhibit Exceptional Electrochemical Stability," *J Electrochem Soc*, no. 160, pp. F1207-F1215, 2013.
- [8] M. Anwar, X. Yan, S. Shen, N. Husnain, F. Zhu, L. Luo and J. Zhang, "Enhanced durability of Pt electrocatalyst with tantalum doped titania as catalyst support," *Int. J. Hydrogen Energy*, no. 42, pp. 30750-30759, 2017.
- [9] Y. Gao, M. Hou, Z. Shao, C. Zhang, X. Qin and B. Yi, "Preparation and characterization of Ti<sub>0.7</sub>Sn<sub>0.3</sub>O<sub>2</sub> as catalyst support for oxygen reduction reaction," *J. Energy Chem*, no. 23, pp. 331-337, 2014.
- [10] J. C. Meier, C. Galeano, I. Katsounaros, A. A. Topalov, A. Kostka, F. Schuüth, and K. J. J. Mayrhofer, "Degradation Mechanisms of Pt/C Fuel Cell Catalysts under Simulated Start-Stop Conditions," *ACS Catalysis*, vol. 2, no. 5, pp. 832-843.
- [11] J. Zhao and X. Li, "A review of polymer electrolyte membrane fuel cell durability for vehicular applications, Degradation modes and experimental techniques," *Energy Convers. Manage*, no. 199, p. 112022, 2019.
- [12] B. G. Pollet, S. S. Kocha and I. Staffell , "B. G. Pollet, S. S. Kocha, I. Staffell, Current status of automotive fuel cells for sustainable transport, Current Opinion in Electrochemistry," no. 16, p. 90–95, 2019.
- [13] Z. Zhang, J. Liu, J. Gu, L. Su and L. Cheng, "An overview of metal oxide materials as electrocatalysts and supports for polymer electrolyte fuel cells," *Energy Environ. Sci*, no. 7, pp. 2535-2558, 2014.
- [14] D. Gubán, I. Borbáth, Z. Pászti, Sajó, E. Drotár, M. Hegedűs and A. Tompos, "Preparation and characterization of novel Ti<sub>0.7</sub>W<sub>0.3</sub>O<sub>2</sub>-C composite materials for Pt-based anode electrocatalysts with enhanced CO tolerance," *Appl. Catal. B: Environ*, no. 174, pp. 455-470, 2015.
- [15] . Á. Vass, I. Borbáth, Z. Pászti, I. Bakos, I. E. Sajó, P. Németh and A. Tompos, "I. E. Sajó, P. Németh, A. Tompos, Effect of Mo incorporation on the electrocatalytic performance of Ti–Mo mixed oxide–carbon composite supported Pt electrocatalysts," *React. Kinet. Mech. Cat*, no. 121, pp. 141-160, 2017.
- [16] D. Gubán, Z. Pászti, I. Borbáth, I. Bakos, E. Drotár, I. Sajó and A. Tompos, "E. Drotár, I. Sajó, A. Tompos, Design and preparation of CO tolerant anode electrocatalysts for PEM fuel cells," *Period. Polytech.-Chem*, no. 60, pp. 29-39, 2016.

- [17] Á. Vass, I. Borbáth, I. Bakos, Z. Pászti, G. Sáfrán and A. Tompos, "Stability issues of CO tolerant Pt-based electrocatalysts for polymer electrolyte membrane fuel cells: comparison of Pt/Ti<sub>0.8</sub>Mo<sub>0.2</sub>O<sub>2</sub>-C with PtRu/C," *React. Kinet. Mech. Cat*, no. 126, pp. 679-699, 2019.
- [18] Á. Vass, I. Borbáth, I. Bakos, Z. Pászti, I. E. Sajó and A. Tompos, "Á. Vass, I. Borbáth, I. Bakos, Z. Pászti, I. E. Sajó, A. Tompos, Novel Pt Electrocatalysts: Multifunctional Composite Supports for Enhanced Corrosion Resistance and Improved CO Tolerance," *Top. Catal*, no. 61, pp. 1300-1312, 2018.
- [19] I. Borbáth, K. Zelenka, Á. Vass, Z. Pászti, G. P. Szijjártó, Z. Sebestyén, G. Sáfrán and A. Tompos, "CO tolerant Pt electrocatalysts for PEM fuel cells with enhanced stability against electrocorrosion," *Int. J. Hydrogen Energy*, no. 46, pp. 13534-13547, 2021.
- [20] M. S. Yazici, S. Dursun, I. Borbáth and A. Tompos, "Reformate gas composition and pressure effect on CO tolerant Pt/Ti<sub>0.8</sub>Mo<sub>0.2</sub>O<sub>2</sub>-C electrocatalyst for PEM fuel cells," *Int. J. Hydrogen Energy*, no. 46, pp. 13524-13533, 2021.
- [21] D. Gubán, A. Tompos, I. Bakos, Á. Vass, Z. Pászti, E. G. Szabó, I. E. Sajó and I. Borbáth, "Preparation of CO-tolerant anode electrocatalysts for polymer electrolyte membrane fuel cells," *Int. J. Hydrogen Energy*, p. 13741-13753, 2017.
- [22] I. Borbáth, E. Tálas, Z. Pászti, K. Zelenka, I. Ayyubov, K. Salmanzade, I. E. Sajó, G. Sáfrán and A. Tompos, "Investigation of Ti-Mo mixed oxide-carbon composite supported Pt electrocatalysts: Effect of the type of carbonaceous materials," *Appl. Catal. A Gen*, no. 620, p. 11815, 2021.
- [23] N. C. Emeka, P. E. Imoisili and T. C. Jen, "Preparation and Characterization of Nb<sub>x</sub>O<sub>y</sub> Thin Films: A Review," *Coatings*, no. 10, p. 1246, 2020.
- [24] A. Mattsson, M. Leideborg, K. Larsson, G. Westin and L. Österlund, "Adsorption and Solar Light Decomposition of Acetone on Anatase TiO<sub>2</sub> and Niobium Doped TiO<sub>2</sub> Thin Films," *J. Phys. Chem. B*, no. 110, pp. 1210-1220, 2006.
- [25] L. Chevallier, A. Bauer, S. Cavaliere, R. Hui, J. Rozière, and D. J. Jones, "Mesoporous Nanostructured Nb-Doped Titanium Dioxide Microsphere Catalyst Supports for PEM Fuel Cell Electrodes," *ACS Appl. Mater. Interfaces*, no. 4, pp. 1752-1759, 2012.
- [26] N. R. Elezović, B. M. Babić, L. Gajić-Krstajić, V. Radmilović, N. V. Krstajić and L. J. Vračar, "Synthesis, characterization and electrocatalytical behavior of Nb-TiO<sub>2</sub>/Pt nanocatalyst for oxygen reduction reaction," *Journal of Power Sources*, no. 195, pp. 3961-3968, 2010.

- [27] T. Do, M. Cai, M. S. Ruthkosky and T. E. Moylan, "Niobium-doped titanium oxide for fuel cell application," *Electrochimica Acta*, no. 55, pp. 8013-8017, 2010.
- [28] A. Bernasik, M. Radecka, M. Rekas and M. Sloma, "Electrical properties of Cr- and Nb-doped TiO<sub>2</sub> thin film," *Appl. Surf. Sci.*, vol. 6, no. 65, pp. 240-245, 1993.
- [29] L. R. Sheppard, T. Bak, J. Nowotny and M. K. Nowotny, "Titanium dioxide for solar-hydrogen V. Metallic-type conduction of Nb-doped TiO<sub>2</sub>," *Int. J. Hydrogen Energy*, no. 32, pp. 2660-2663, 2007.
- [30] A. M. Ruiz, G. Dezanneau, J. Arbiol, A. Cornet and J. R. Morante, "Insights into the Structural and Chemical Modifications of Nb Additive on TiO<sub>2</sub> Nanoparticles," *Chem. Mater.*, no. 16, pp. 862-871, 2004.
- [31] T. Anukunprasert, C. Saiwan and E. Traversa, "The development of gas sensor for carbon monoxide monitoring using nanostructure of Nb-TiO<sub>2</sub>," *Sci. Tech. Adv. Mater.*, no. 6, pp. 359-363, 2005.
- [32] E. Traversa, M. L. Di Vona, S. Licocchia, M. Sacerdoti, M. C. Carotta, L. Crema and G. Martinelli, "Sol-Gel Processed TiO<sub>2</sub>-Based Nano-Sized Powders for Use in Thick-Film Gas Sensors for Atmospheric Pollutant Monitoring," *J. Sol-Gel Sci. Technol.*, no. 22, pp. 167-179, 2001.
- [33] M. Valigi, D. Cordischi, G. Minelli, P. Natale, P. Porta and C. P. Keijzers, "A Structural, Thermogravimetric, Magnetic, Electron Spin Resonance, and Optical Reflectance Study of the NbO<sub>x</sub>-TiO<sub>2</sub> System," *J. Solid State Chem.*, no. 77, pp. 255-263, 1988.
- [34] K. Zakrzewska, M. Radecka and M. Rekas, "Effect of Nb, Cr, Sn additions on gas sensing properties of TiO<sub>2</sub> thin films," *Thin Solid Films*, no. 310, pp. 161-166, 1997.
- [35] J. H. Kim, G. Kwon, H. Lim, C. Zhu, H. You and Y. T. Kim, "Effects of transition metal doping in Pt/M-TiO<sub>2</sub> (M = V, Cr, and Nb) on oxygen reduction reaction activity," *J. Power Sources*, no. 320, pp. 188-195, 2016.
- [36] K. Sasaki, L. Zhang and R. R. Adzic, "Niobium oxide-supported platinum ultra-low amount electrocatalysts for oxygen reduction," *Phys. Chem. Chem. Phys.*, no. 10, pp. 159-167, 2008.
- [37] N. R. Elezovic, B. M. Babic, V. R. Radmilovic, L. M. Vracar and N. V. Krstajic, "Nb-TiO<sub>2</sub> supported platinum nanocatalyst for oxygen reduction reaction in alkaline solutions," *Electrochimica Acta*, no. 56, pp. 9020-9026, 2011.
- [38] S. Sun, G. Zhang, X. Sun, M. Cai and M. Ruthkosky, "Highly Stable and Active Pt/Nb-

- TiO<sub>2</sub> Carbon-Free Electrocatalyst for Proton Exchange Membrane Fuel Cells," *Journal of Nanotechnology*, p. 8, 2012.
- [39] A. Bauer, K. Lee, C. Song, Y. Xie, J. Zhang and R. Hui, "Pt nanoparticles deposited on TiO<sub>2</sub> based nanofibers: Electrochemical stability and oxygen reduction activity," *J. Power Sources*, no. 195, pp. 3105-3110, 2010.
- [40] V. K. V. P. Srirapu, A. Kumar, P. Srivastava, R. N. Singh and A. S. K. Sinha, "Nanosized CoWO<sub>4</sub> and NiWO<sub>4</sub> as efficient oxygen-evolving electrocatalysts," *Electrochim. Acta*, no. 209, pp. 75-84, 2016.
- [41] J. Wang, H. Jang, G. Li, M. G. Kim, Z. Wu and X. Liu, "Efficient electrocatalytic conversion of N<sub>2</sub> to NH<sub>3</sub> on NiWO<sub>4</sub> under ambient conditions," *Nanoscale*, no. 12, pp. 1478-1483, 2020.
- [42] R. R. Adzic and N. S. Marinkovic, "Electrocatalysts for alcohol oxidation in fuel cells," *US Patent*, vol. 6, no. 183, p. 894, 2001.
- [43] M. Shi, X. Tong, W. Li, J. Fang, L. Chen and C. Ma, "Enhanced electrocatalytic oxygen reduction on NiWO<sub>x</sub> solid solution with induced oxygen defects," *ACS Appl. Mater. Interfaces*, no. 9, p. 34990–35000, 2017.
- [44] A. Halder, M. Zhang and Q. Chi, "Electrocatalytic Applications of Graphene-Metal Oxide Nanohybrid Materials," *Advanced Catalytic Materials - Photocatalysis and Other Current Trends*, no. 14, pp. 379-413, 2016.
- [45] K. C. Neyerlin, W. Gu, J. Jorne and H. A. Gasteiger, "Study of the Exchange Current Density for the Hydrogen Oxidation and Evolution Reactions," *J. Electrochem. Soc.*, no. 154, pp. 631-635, 2007.
- [46] W. Sheng, H. A. Gasteiger and Y. Shao-Horn, "Hydrogen Oxidation and Evolution Reaction Kinetics on Platinum: Acid vs Alkaline Electrolytes," *J. Electrochem. Soc.*, no. 157, pp. B1529-B1536, 2010.
- [47] C. M. Zalitis, J. Sharman, E. Wright and A. R. Kucernak, "Properties of the hydrogen oxidation reaction on Pt/C catalysts at optimised high mass transport conditions and its relevance to the anode reaction in PEMFCs and cathode reactions in electrolyzers," *Electrochim. Acta*, no. 176, pp. 763-776, 2015.
- [48] O. Guillén-Villafuerte, G. García, J. L. Rodríguez, E. Pastor, R. Guil-López, E. Nieto and J. L. G. Fierro, "Preliminary studies of the electrochemical performance of Pt/X@MoO<sub>3</sub>/C (X= Mo<sub>2</sub>C, MoO<sub>2</sub>, MoO) catalysts for the anode of a DMFC: Influence of the Pt loading

- and Mo-phase," *Int. J. Hydrogen Energy*, no. 38, pp. 7811-7821, 2013.
- [49] P. Justin and G. R. Rao, "Methanol oxidation on MoO<sub>3</sub> promoted Pt/C electrocatalyst," *Int. J. Hydrogen Energy*, no. 36, pp. 5875-5884, 2011.
- [50] A. C. C. Tseung, P. K. Shen and K. Y. Chen, "Precious metal/hydrogen bronze anode catalysts for the oxidation of small organic molecules and impure hydrogen," *J Power Source*, no. 61, pp. 223-225, 1996.
- [51] J. Shim, C. R. Lee, H. K. Lee, J. S. Lee and E. J. Cairns, "Electrochemical characteristics of Pt-WO<sub>3</sub>/C and Pt-TiO<sub>2</sub>/C electrocatalysts in a polymer electrolyte fuel cell," *J Power Sources*, no. 102, pp. 172-177, 2001.
- [52] X. Cui, L. Guo, F. Cui, Q. He and J. Shi, "Electrocatalytic activity and CO-tolerance properties of mesostructured Pt/WO<sub>3</sub> composite as an anode catalyst for PEMFCs," *J. Phys. Chem. C*, no. 113, pp. 4134-4138, 2009.
- [53] Á. Vass, I. Borbáth, Z. Pászti, I. Bakos, I. E. Sajó, P. Németh and A. Tompos, "Effect of Mo incorporation on electrocatalytic performance of Ti-Mo mixed oxide-carbon composite supported Pt electrocatalysts," *React Kinet Mech Cat*, vol. 121, pp. 141-160, 2017.
- [54] "T.T. Nguyen, V.T.T. Ho, C.J. Pan, J.Y. Liu, H.L. Chou, J. Rick, W.H. Su, B.J. Hwang, Synthesis of Ti<sub>0.7</sub>Mo<sub>0.3</sub>O<sub>2</sub> supported- Pt nanodendrites and their catalytic activity and stability for oxygen reduction reaction," *Appl. Catal. B: Environ.*, no. 154-155, pp. 183-186, 2014.
- [55] "C.M. Zalitis, J. Sharman, E. Wright, A.R. Kucernak, Properties of the hydrogen oxidation reaction on Pt/C catalysts at optimised high mass transport conditions and its relevance to the anode reaction in PEFCs and cathode reactions in electrolyzers. Electr".
- [56] D. Guban, Preparation of CO-tolerant anode-side electro catalysts for polymer electrolyte membrane fuel cells, Budapest, Hungary: Budapest University of Technology and Economics, 2005.